**Article:**
Tessin, A, Maerz, C orcid.org/0000-0003-2558-4711, Kędra, M et al. (5 more authors) (2020) Benthic phosphorus cycling within the Eurasian marginal sea ice zone. Philosophical Transactions of the Royal Society A: Mathematical, Physical and Engineering Sciences, 378 (2182). 20190358. ISSN 1364-503X

https://doi.org/10.1098/rsta.2019.0358

PHILOSOPHICAL TRANSACTIONS
OF THE ROYAL SOCIETY A
MATHEMATICAL, PHYSICAL AND ENGINEERING SCIENCES

# Benthic phosphorus cycling within the Eurasian marginal sea ice zone

| | |
|---|---|
| Journal: | *Philosophical Transactions A* |
| Manuscript ID | RSTA-2019-0358.R1 |
| Article Type: | Research |
| Date Submitted by the Author: | n/a |
| Complete List of Authors: | Tessin, Allyson; Kent State University, Department of Geology ; University of Leeds<br>Maerz, Christian; University of Leeds Faculty of Environment, School of Earth and Environment<br>Kedra, Monika; Polish Academy of Sciences Institute of Oceanology<br>Matthiessen, Jens; Alfred Wegener Institute for Marine and Polar Research<br>Morata, Nathalie; Akvaplan-niva AS; Ifremer Centre de Brest<br>Nairn, Michael; Cardiff University School of Earth and Ocean Sciences<br>O'Regan, Matthew; Stockholm University Department of Geological Sciences<br>Peeken, Ilka; Alfred Wegener Institute for Marine and Polar Research |
| Issue Code (this should have already been entered and appear below the blue box, but please contact the Editorial Office if it is not present): | ARCTIC-CHANGE |
| Subject: | Biogeochemistry < EARTH SCIENCES |
| Keywords: | Barents Sea slope, Yermak Plateau, sediments, pore waters, nutrient cycling |
| | |

## Author-supplied statements

Relevant information will appear here if provided.

### *Ethics*

*Does your article include research that required ethical approval or permits?:*
This article does not present research with ethical considerations

*Statement (if applicable):*
CUST_IF_YES_ETHICS :No data available.

### *Data*

*It is a condition of publication that data, code and materials supporting your paper are made publicly available. Does your paper present new data?:*
Yes

*Statement (if applicable):*
The datasets supporting this article have been uploaded to Pangaea. Additional data used in this paper are found in [34,37].

### *Conflict of interest*

I/We declare we have no competing interests

*Statement (if applicable):*
CUST_STATE_CONFLICT :No data available.

### *Authors' contributions*

This paper has multiple authors and our individual contributions were as below

*Statement (if applicable):*
AT and CM were responsible for the design of this project. CM, MK, NM, MN, JM, MO, and IP were involved in sample collection. AT, CM, MK, and NM contributed to data production. All authors contributed to the data interpretation, drafting, revising, and final approval of the manuscript.

PHILOSOPHICAL TRANSACTIONS A

Phil. Trans. R. Soc. A.
doi:10.1098/not yet assigned

# Benthic phosphorus cycling within the Eurasian marginal sea ice zone

**Allyson Tessin[*,1,2], Christian März[2], Monika Kędra[3], Jens Matthiessen[4], Nathalie Morata[5,6], Michael Nairn[7], Matthew O'Regan[8], Ilka Peeken[4]**

[1] Department of Geology, Kent State University, Kent, OH, USA.
[2]School of Earth and Environment, University of Leeds, Leeds, UK.
[3] Institute of Oceanology Polish Academy of Sciences, Sopot, Poland.
[4] Alfred-Wegener-Institut Helmholtz-Zentrum für Polar- und Meeresforschung, Bremerhaven, Germany.
[5]Akvaplan-niva AS, Fram Centre, Tromsø, Norway.
[6]CNRS, Imov Brest, IRD, Ifremer, LLEMAR Plouzane, France.
[7]School of Earth and Ocean Sciences, Cardiff University, Cardiff, UK.
[8]Department of Geological Sciences, Stockholm University, Stockholm, Sweden.

**Keywords:** Barents Sea slope, Yermak Plateau, sediments, porewaters, nutrient cycling



## Summary

The Arctic Ocean region is currently undergoing dramatic changes, which will likely alter the nutrient cycles that underpin Arctic marine ecosystems. Phosphate is a key limiting nutrient for marine life but gaps in our understanding of the Arctic phosphorus (P) cycle persist. In this study, we investigate the benthic burial and recycling of phosphorus using sediments and porewaters from the Eurasian Arctic margin, including the Barents Sea slope and the Yermak Plateau. Our results highlight that P is generally lost from sediments with depth during organic matter respiration. On the Yermak Plateau, remobilization of P results in a diffusive flux of P to the seafloor of between 96 and 261 $\mu$mol $m^{-2}$ $yr^{-1}$. On the Barents Sea slope, diffusive fluxes of P are much larger (1736 to 2449 $\mu$mol $m^{-2}$ $yr^{-1}$) but these fluxes are into near surface sediments rather than to the bottom waters. The difference in cycling on the Barents Sea slope is controlled by higher fluxes of fresh organic matter and active iron cycling. As changes in primary productivity, ocean circulation, and glacial melt continue, benthic P cycling is likely to be altered with implications for P imported into the Arctic Ocean Basin.

## Introduction

The Arctic Ocean is experiencing some of the fastest and most drastic changes on Earth in response to anthropogenic climate change, including rapid reduction of sea ice cover and thickness [1], retreat of marine

*Author for correspondence (allyson.tessin@usm.edu).
†Present address: [1]*Division of Marine Science, University of Southern Mississippi, Kiln, MS, USA*

terminating glaciers, changing ocean circulation patterns [2,3], and ocean warming [4]. These changes are affecting the entire Arctic marine ecosystem, including the primary producers at the base of the food web. Primary productivity in the Arctic can be either light or/and nutrient limited [5,6]. As sea ice continues to retreat, light limitations will be reduced followed by anticipated increase of primary production [7]. Nutrient availability is likely to change in response to enhanced utilization from primary productivity as sea ice retreats and to changes in nutrient inputs due to changes in ocean circulation patterns, stratification, and meltwater fluxes from land [6].

An understanding of the evolving sources and sinks of phosphate is necessary for predicting future changes in the Arctic primary productivity, which underpins the health of the entire Arctic ecosystem and can drive climate feedbacks associated with carbon burial. Phosphate plays a key role in marine environments [8,9], however gaps in our understanding of the marine phosphate cycle persist [10]. Phosphate is commonly considered to be the "ultimate" limiting nutrient in the ocean over long timescales [8] due to its long residence times and the possibility that N deficits can be offset by N fixation. The specific ratios of available nutrients can also affect the distribution and biogeochemical roles of plankton, as many plankton are adapted to relative differences in P and N availability [10,11].

Dissolved P is delivered to the oceans from land by rivers, dust, and ice-rafted debris and removed from seawater through sedimentary burial [12,13]. Mass balanced transport estimates of phosphate for the entire Arctic Ocean indicate that the Arctic is a net exporter of dissolved inorganic phosphorus to the North Atlantic [14]. Riverine inputs of phosphate to the Arctic cannot explain the missing source of phosphate, demonstrating that the P cycle within the Arctic remains poorly understood [15]. One possible source of P is glacial melt. Recent work from Greenland indicates that glacial melt represents a significant source of this missing P [16].

Phosphorus cycling in the benthic environment is also important, because phosphorus can be sequestered in sediments or recycled back into the water column. As organic matter is remineralized within sediments, dissolved inorganic and organic phosphorus is released into sediment pore waters. These dissolved phosphorus phases may be released to bottom waters by diffusive fluxes from the seafloor or sequestered via sorption on minerals such as Fe and Mn oxides or authigenic mineral formation such as carbonate fluorapatite and vivianite [17–19]. Adsorption and co-precipitation with Fe oxides may be especially important in polar continental margins, which may have large fluxes of reactive Fe from terrestrial glacial melt [20–23].

Here we focus on cores collected on the Arctic Margin north of Svalbard, including the Barents Sea slope, the Sofia Basin, and the Yermak Plateau, to investigate benthic controls on phosphate cycling. Our main aim was to investigate the benthic burial and recycling of P in the Arctic Ocean. We present paired pore water and sediment data to investigate the controls on phosphorus fluxes from the seafloor to the water column. Phosphorus speciation data is also paired with Fe speciation results to evaluate the relationship between Fe minerals and phosphate sequestration in the sediments.

# Study Site

This study focuses on the marginal sea ice zone north of the Svalbard archipelago (Figure 1). Study locations from the Barents Sea slope, north of Spitsbergen, range from 481 to 1852 m water depth. The Yermak Plateau is a bathymetric feature to the northeast of Svalbard and is separated from the northern Barents Sea slope by the Sofia Basin. Estimates of recent sedimentation rates are generally low and similar in both the northern Barents Sea (0.5-1.0 mm/ $yr^{-1}$; [24]) and the Yermak Plateau (0.7 mm/$yr^{-1}$; [25]). Study locations from the Yermak Plateau range from 817 to 1523 m water depth, and the study location from the Sofia Basin is 2175 m. The region is situated at the entrance of the Arctic Ocean, where Atlantic water flows into the Central Arctic basin. The West Spitsbergen Current (WSC) carries nutrient-rich, warm, saline ($T \geq 2$°C, S ≥ 34.88 psu) [26] Atlantic waters northwards in the eastern Fram Strait. Between 78° and 80° N, the WSC splits, with the main branch flowing along the western and then northern continental margin of Spitsbergen [27–31]. During transit northwards, water temperatures and salinities in the WSC decrease by 0.20°C/100 km and 0.010 psu/100 km [32]. This current continues along the eastern margin of the Eurasian Basin.

The study area is sea ice covered during the winter with the sea ice maximum being reached in March (Figure 1). In the spring, sea ice begins to melt, and during the summer the region is located within the marginal sea ice zone, which is the transition between the open ocean and sea ice. The sea ice minimum is reached in September. Sedimentary Fe cycling was previously examined at these core locations (Tessin et al., in revision). This study highlighted that in the Barents Sea slope region, reactive Fe was remobilized within sediments and shuttled away region. On the Yermak Plateau and Sofia Basin, reactive Fe accumulated in sediments with no evidence for remobilization. The main driver of these differences was higher oxidant demand within Barents Sea slope sediments associated with higher fluxes of organic carbon to the seafloor, which fueled more Fe reduction and remobilization, resulting in near surface accumulation or sediment loss. Conversely, low oxidant demand within the Yermak Plateau and Sofia Basin sediments resulted in enrichments of reactive Fe within the upper 30 cm.

# Materials and Methods

Sediment samples were collected with the RV *Polarstern* using a multicorer during spring 2015, May/June, as part of the Transitions in the Seasonal Sea Ice Zone (TRANSSIZ) expedition PS92 ([33]; Figure 1). Core top results from nine locations are presented (Table 1). Downcore results were additionally produced on representative cores taken from five sites on the Barents Sea slope and Yermak Plateau (PS92/019-19, 27-15, 39-5, 46-16, and 56-5; Table 1). Cores were sliced onboard at 1 cm resolution and frozen at -20˚C. Samples were subsequently freeze-dried and powdered in an agate mortar and pestle in the laboratory.

A sample split from cores 19-19, 27-15, 39-05, 46-15, and 56-05 was prepared for wavelength dispersive X-ray fluorescence (XRF) by borate glass bead fusion. The XRF analyses of total Fe, Al, and P were performed using a Philips PW-2400 WD-XRF spectrometer calibrated with 53 geostandards at the University of Oldenburg (for detailed method description, see [34]). A sediment split from all cores was analyzed for Fe-bound phosphorus after extraction by citrate-dithionite-bicarbonate (CDB; pH=8.0) for 8 hours at room temperature [35]. Extracted P concentrations were determined by inductively coupled plasma-optical emission spectrometry (Thermo iCAP 7400 ICP-OES) at the University of Leeds (for detailed method description, see ([36])). The most reactive Fe oxyhydroxides (OHO; i.e. ferrihydrite) have been previously extracted and measured [37] using an ascorbate extraction [38].

Carbon concentrations were measured on a LECO CS244 carbon analyser at the University of Newcastle for all cores. Total organic and inorganic carbon were determined using paired acidified (organic) and unacidified (total) carbon measurements. In preparation for analysis of total organic carbon, samples were acidified in 5% HCl until all the carbonate was removed. Dried, acidified samples were powdered and homogenized in an agate mortar and pestle prior to analysis. Chlorophyll *a* (Chl *a*) concentrations were analyzed on samples from all cores except 40-01 and 56-05 fluorometrically following methods described in [39] and results for most locations were previously published in [40,41].

Pore waters were extracted onboard using Rhizon samplers (Rhizosphere; 0.15 μm pore size) with vacuum applied by plastic syringes with wooden stoppers [42]. Samples were collected from all cores at resolutions between 1 and 5 cm, with decreasing resolution downcore. Bottom waters were sampled from the water overlying the sediments within the multicorer. Pore waters were acidified with ultrapure HCl and stored at 4˚C. Pore waters were then diluted 1:1 with MQ water and analyzed for major element composition, including Fe and P, by inductively coupled plasma-optical emission spectrometry (Thermo iCAP 7400 ICP-OES) at the University of Leeds. An internal standard spiked with Y was added to each sample to monitor the

precision of Fe and P measurements via ICP-OES. Analytical precision (2 standard deviations of the measured value/reported value) for Fe and P were ±1.91 and ±2.53, respectively.

Diffusive fluxes were calculated using Fick's first law of diffusion (Equation 1) assuming steady state conditions from pore water P results under the assumption that the P pool was all in the species $HPO_4^{2-}$. The concentration gradient was determined from the sediments to the bottom waters with the exception of cores that have no gradient across the sediment water interface. For these cores (19-19, 27-15, and 31-13), a diffusive flux of P was calculated into the oxic layer.

$$J = \Phi \times D_s \times \frac{\partial C}{\partial x} \quad \text{(Equation 1)}$$

Where J is the diffusive flux, $D_s$ is the sedimentary diffusion constant, Φ is the porosity, and ∂C/∂x is the concentration gradient. Without direct measurements for porosity, a conservative value of 0.8 was chosen following [43].

The sediment diffusion constant was calculated with the empirical equation of Ullman and Aller [44](Equation 2), which takes into consideration sediment tortuosity. A diffusive molecular coefficient, Dm, of 0.0134 $m^2 yr^{-1}$ was used for $HPO_4^{2-}$ at 4°C.

$$D_s = \Phi^{n-1} \times D_m \text{ (Equation 2)}$$

Where $D_s$ is the sedimentary molecular diffusion constant, Φ is the porosity, n is a correction factor (such that n = 2 when porosity is > 0.7).

# Results

On the shallowest core location on the Barents Sea slope (19-19), P/Al (presented as weight percent ratios) is elevated within the top 7 cm (up to 0.034) with values of 0.010 for the rest of the core (Figure 2). In a deeper Barents Sea slope core (27-15), P/Al decreases from 0.015 at the sediment water interface to 0.012 at 8.5 cm. Below this, P/Al increases to 0.014 and then decreases to the base of the core (0.012). In cores from the Yermak Plateau 39-5 and 46-15, P/Al decreases from 0.014 to 0.012. The P/Al ratio also decreases in the other Yermak Plateau core (56-5) from 0.013 to 0.007 with the exception of an increase in the relative P concentration at 1.5 cm. The trends in P/Fe are generally similar to P/Al with values ranging between 0.015 and 0.044 (Figure 2).

Core top TOC values range from 0.53 to 1.61%. In the five cores with downcore TOC records, TOC decreases with depth (Figure 3). Organic carbon to phosphorus ($C_{org}$/P) ratios (presented as weight percent

ratios) broadly decrease with depth in all cores except 19-19, with core top values from 10.0 to 12.9 and values below the surface sediments as low as 5.2 (Figure 3). In core 19-19, $C_{org}/P$ values decrease from the surface (13.1) to minimum values at 2.5 cm (6) below the sediment water interface coincident with the maximum P/Al values before increasing again to an average value of 17.6. Concentrations of Chl *a* in the surface sediments range from 0.04 to 0.71 $\mu g/g$, with higher concentrations of the Barents Sea slope (Table 2). Iron bound phosphorus ranges between 0.003% and 0.034% (Table 2; Figure 4) with the highest concentrations in the top 5 cm of core 19-19 and the lowest concentrations in sediments below 5 cm in core 19-19 and in the other Barents Sea slope cores (27-15 and 31-13). The Fe bound P represents between 3% and 14% of the P pool.

In the Yermak Plateau cores (39-5, 46-15, and 56-5), porewater P increases downcore with maximum concentrations of 5.39 $\mu$mol, 4.06 $\mu$mol, and 4.84 $\mu$mol, respectively (Figure 5). In the Barents Sea slope cores (19-19 and 27-15), the concentration of porewater P in the top 2 cm is less than or equal to seawater P (0.00 and 0.85 $\mu$mol, respectively). In both Barents Sea Slope cores, porewater P increases sharply at 2 cm before stabilizing to average concentrations of 31.79 $\mu$mol and 3.56 $\mu$mol. Porewater Fe/P (weight:weight) ratios are plotted in Figure 5. Most samples have values of <3.3, with the exception of samples from core 19-19, which has values up to 25.2. Calculated diffusive fluxes range from 117 to 2449 $\mu mol\ m^{-2}\ yr^{-1}$ (Table 3). At all core sites on the Yermak Plateau (39-5, 40-01, 43-20, 46-15, 56-5) and Sofia Basin (47-20) there is a flux of P from the sediments into the bottom waters across the sediment water interface. Conversely, at the Barents Sea slope core sites (19-19, 27-15, 31-13), there is no flux of P across the sediment water interface, but a flux from deeper sediments into a near surface layer (0-3 cm). The flux of P into the bottom waters on the Yermak Plateau and Sofia Basin are an order of magnitude lower than the Barents Sea slope fluxes from deeper sediments into a near surface layer.

# Discussion

At all core locations, P decreases with depth as compared to both Al and Fe, indicating that relatively less P is preserved at depth than is originally deposited at the seafloor (Figure 2). Total organic carbon within sediments also decreases downcore, indicating that the patterns of P loss are controlled by the remineralization of organic matter. This would result in a loss of both P and C from the sediments and release of dissolved P to the porewaters [45–47]. Ratios of $C_{org}/P$ decrease downcore, illustrating that P losses are smaller relative to organic carbon with increasing depth. Organic matter respiration appears to have a more significant effect on the organic C pool than the P pool. This is to be expected, since organic bound P represents a small portion of the total P pool, unlike the measured organic carbon. The preferential loss of

organic C relative to P may also suggest that P released to the pore waters is being adsorbed onto mineral phases and/or precipitating as authigenic minerals rather than being lost from the sediments [17–19] or that utilization by benthic organisms affects the C and P pools differently.

Porewater P concentrations are, generally, elevated in the sediments relative to bottom waters (Figure 5). On the Yermak Plateau, P/Al ratios generally decrease from the surface to the deeper sediments (Figure 2), coincident with a gradual increase in porewater P concentrations (Figure 5), supporting that P is being lost from the solid phase and released to porewaters. The gradient of porewater P crosses the sediment water interface, indicating a diffusive flux of P from the sediments to the bottom waters. Porewater P continues to increase in the core with depth, suggesting continued release of dissolved P. Sequestration of P as authigenic carbonate fluorapatite (CFA) has been observed in many continental margin settings (i.e. [48]). While this process may be occurring on the Yermak Plateau, CFA precipitation does not appear to keep pace with P release.

Conversely, on the shallow Barents Sea slope, P/Al ratios are elevated within a near surface sediment layer between 0 and 5 cm. Porewater P profiles on the Barents Sea slope (19-19) are characterized by zero to low concentrations in the upper 2 cm and a rapid increase in P concentrations below this depth. These profiles indicate that P is released to porewaters within sediments deeper than 5 cm and porewater P is sequestered in near surface sediments. Benthic P cycling on the deeper Barents Sea Slope is intermediate to the Yermak Plateau and shallow Barents Sea slope. The porewater results from the deeper Barents Sea Slope (27-15) are similar to core 19-19, despite the lack of sedimentary evidence for an Fe- and P-rich near surface layer, perhaps suggesting that Fe and P accumulated near the surface but were later physically and/or biogeochemically remobilized. Elevated but stable concentrations of porewater P at both sites below 10 cm may indicate CFA precipitation within sediments but further P extractions and porewater results (F concentrations) would be required to directly test this. Diffusive fluxes of P were calculated based on pore water total dissolved P profiles. The calculated benthic fluxes illustrate that the flux of P into the near surface sediment layers on the Barents Sea slope is an order of magnitude higher than the flux of P to bottom waters in Yermak Plateau sites (Figure 6).

The accumulation of P in the near surface oxic layer in core 19-19 co-occurs with Fe-rich sediments at this location [37] suggesting that P is sorbing onto Fe oxide and oxyhydroxide minerals (Fe OHO) within near surface sediments. The role of Fe in binding sedimentary P has been well established based on the observation that porewater P can be trapped within sediments through sorption to Fe OHO surfaces and/or co-precipitation with dissolved $Fe^{2+}$ [49–52].

To evaluate the relationship between benthic Fe and P cycling, the amount of P bound to Fe was quantified (Figure 4) and compared to the concentration of the most reactive Fe OHO, ferrihydrite. Ferrihydrite has the highest P adsorption potential and fastest adsorption rates compared to other Fe minerals because it is poorly crystalline and has a higher surface site density (Wang et al., 2013). All samples contained Fe bound P, indicating that some P is sorbed to Fe minerals in all locations and at all depths. In most samples, Fe bound P represented less than 10% of the total P pool (Table 2). Higher concentrations (up to 15% of the P pool) were measured within the Fe-rich, near surface sediments of core 19-19 [37].

Within every core, the concentration of Fe bound P and ascorbate extractable Fe covary (Figure 4). However, different relationships exist spatially between these cores. On the Barents Sea slope, higher concentrations of Fe bound P are associated with relatively lower concentrations of Fe OHO (Figure 4). This relationship indicates that P sequestration is more efficient on the Barents Sea slope, where cycling of Fe and P are more active (Figure 5; Tessin et al., in revision). The efficiency of P sequestration on the Barents Sea slope prevents any flux of P to the bottom waters. Conversely, the less efficient P sequestration by Fe minerals on the Yermak Plateau results in a loss of dissolved P from the sediments to the bottom waters, regardless of higher concentrations of reactive Fe in many of the sediments.

The difference in benthic Fe and P cycling between the shallow Barents Sea Slope and the Yermak Plateau is likely associated with differences in fluxes of fresh organic matter [53]. Higher fluxes of fresh organic matter might be expected on the Barents Sea slope which is located in the productive marginal sea ice zone, while the Yermak Plateau is covered with sea ice longer during the year. In addition, the Barents Sea slope is influenced by the core of the Atlantic water inflow ([54] and references therein), which generally supports higher primary production in this region [55,56]. Within the studied cores, surface Chl *a* concentrations, indicate that the Yermak Plateau sediments have a lower concentration of fresh organic matter than the Barents Sea slope ([33,57]; Figure 6). Sediments from core 19-19 also have the highest TOC concentrations (up to 1.6%). However, in the neighboring core 27-15, some of the lowest TOC concentrations (<1%) are found (Figure 6). This may indicate that the deep Barents Sea slope has been organic carbon starved but is now receiving large fluxes of fresh, organic matter. Conversely, it may suggest that because TOC includes OC from multiple sources, it is a poor proxy for the flux of labile organic matter.

The higher fluxes of labile organic matter to the seafloor on the Barents Sea slope would lead to higher levels of organic matter respiration within the sediments and a richer benthic community that would likely enhance OM usage, respiration, and remineralization. Higher rates of respiration will result in higher fluxes of nutrients to the porewaters from respired organic matter. Additionally, respiration consumes oxygen within

the porewaters. Once most of the oxygen is consumed, microbial metabolisms that use other electron acceptors (e.g. $Fe^{3+}$) dominate [58]. $Fe^{2+}$ from these anaerobic sediments diffuse upwards from below, providing a source of Fe for co-precipitation with P. Orange lines in Figure 5 indicate the depth at which Fe precipitates in the sediments from $Fe^{2+}$ diffusing upwards.

On the Barents Sea slope, the transition depth from Fe reduction to Fe OHO precipitation is coincident with elevated dissolved P concentrations (Figure 5). Conversely, on the Yermak Plateau, there is no evidence for Fe reduction within the sediment cores. In summary, the higher fluxes of labile organic matter to the Barents Sea slope, fuels both the higher release of P to porewaters and the active redox cycling that results in the trapping of this P in surface sediments.

The importance of the active reduction and reprecipitation of Fe is highlighted by the Yermak Plateau sediments. While these sediments also contain significant amounts of reactive Fe (Tessin et al., in revision; Figure 4), P does not sorb efficiently enough to these mineral surfaces to stop the flux of P from the seafloor. This may be due to the importance of co-precipitation of P with Fe, rather than sorption of porewater P on pre-existing Fe OHO. One explanation for the low efficiency of P sorption in the Yermak Plateau is that these "preformed" Fe OHO may have decreased adsorption capacity due to pre-sorbed organic matter blocking the mineral surfaces [59].

Ratios of porewater Fe:P can be used to investigate whether porewater conditions are appropriate for P binding. The predominant surface complexation ratio of Fe:P on Fe OHO is 2 mol:mol, which corresponds to a mass ratio of 3.6 [60–62]. It has been proposed that if the porewater $Fe^{2+}$:P ratio is <3.6, the recently formed Fe OHO is not sufficient to bind all the diffusing P resulting in a flux of P to the bottom waters [63]. The porewaters in core 19-19 have high Fe:P ratios (up to 25), which supports the argument that a sufficient flux of Fe is diffusing into the surface layer to trap all P. In core 27-15, values of Fe:P are low, however, significant data are lacking because Fe in porewaters was below detection limits. Within Yermak Plateau sediments, Fe:P ratios are also below 3.6, indicating that the flux of Fe is too low for efficient P binding, despite the abundance of reactive Fe minerals within the sediments.

As a whole, our results indicate that locations underlying more productive surface waters, such as the Barents Sea slope, are characterized by active sedimentary biogeochemical cycling, which results in accumulation of P within near surface sediments. While P is currently sequestered in Barents Sea slope sediments, it is also important to note that our pore water results capture transient conditions that may not persist over longer timescales, especially as the Arctic is currently undergoing rapid changes, which are likely to affect P cycling in the region. The delivery of reactive organic matter to the seafloor acts as a control on

benthic phosphorus cycling both by delivering organic bound phosphorus and by increasing the oxidant demand within sediments, fueling reduction and remobilization of reactive Fe. Changes in sea ice extent and nutrient availability are likely to alter the surface primary productivity and, subsequently, the flux of fresh organic matter to the seafloor. Currently, Chl *a* derived primary productivity is increasing in the Barents Sea and Eurasian Arctic [7]and this region is arguably experiencing the most rapid increases in Chl *a* derived primary productivity (Frey et al., 2018). Models suggest that some of the largest increases in primary productivity in the future will occur on the Eurasian perimeter, including the northern Barents Sea [64,65]. If these predictions are proven correct, it would be expected that the flux of P to the seafloor would increase in this region, as the depth of Fe reduction shoals within the sediments remobilizing sorbed P. The availability of reactive Fe is a main control on benthic P recycling and therefore, changes in the delivery of reactive Fe to the seafloor will impact benthic P cycling. Within polar regions, glacial melt [20–23] and ice rafted debris ([66]) act as sources of of reactive Fe. Therefore, future chances in meltwater and ice rafting are likely to impact both benthic Fe and P cycling.

# Conclusions

This study investigated benthic cycling of P on the Eurasian Arctic margin. Combined sediment and pore water geochemical data shed light on the controls of P burial and recycling in Barents Sea slope and Yermak Plateau sediments. These results indicate that fluxes of P are controlled by delivery of fresh organic matter and the precipitation of fresh Fe minerals within sediments. Porewater results from the Barents Sea slope cores indicate high P fluxes into near surface (0-5 cm) sediment layers. On the shallow slope, this pattern can be clearly explained by the co-precipitation of P with Fe OHO minerals in Fe-rich, near surface sediments. Results from the deeper slope are more ambiguous since pore waters indicate P trapping in the upper 2 cm of sediments, but an obvious Fe and P-rich oxic layer is not observed. However, the ratio of $Fe_{ox}$ to Fe-bound P still hints at P trapping within this layer.

In contrast, Yermak Plateau cores exhibit trends characteristic of P loss due to organic matter remineralization resulting in a small flux of P from the seafloor into the bottom waters. While these cores all contain reactive Fe and Fe-bound P, P sequestration is not efficient. In all of the Yermak Plateau cores, porewater Fe/P ratios are lower than 3.6, suggesting that dissolved Fe concentrations are insufficient to bind dissolved P. This result highlights that the presence alone of reactive Fe oxide minerals is not sufficient to sequester P and that efficient binding of P requires co-precipitation of Fe and P.

In response to anthropogenic warming, sea ice is expected to retreat further and patterns of surface ocean primary productivity are expected to change, leading to changes in the patterns of P burial and recycling as well. Altered patterns of the delivery and recycling of reactive Fe within sediments will be of primary importance to future benthic P cycling. Increased delivery of labile organic matter in response to elevated surface productivity, will increase the oxidant demand and Fe remobilization within sediments. These changes may result in conditions on the Yermak Plateau shifting towards those observed on the Barents Sea slope. Increased organic carbon fluxes on the Barents Sea slope may result in large fluxes sedimentary fluxes of P to bottom waters, as a large stock of P has been accumulated in near surface sediments.

# Additional Information

**Information on the following should be included wherever relevant.**

### Acknowledgments
The TRANSSIZ cruise (Transitions in the Arctic Seasonal Sea Ice Zone; PS92) was initiated and co-organized by the Arctic in Rapid Transition (ART) network. The authors thank the crew of RV Polarstern and chief scientist Ilka Peeken. We would like to thank Andy Connelly and Stephen Reid for analytical support.

### Funding Statement
This study was funded by the PACES (Polar Regions and Coasts in a Changing Earth System) programme of the Helmholtz Association (Grant No AWI_PS92_00). AT received funding for this project from the European Union's Horizon 2020 research and innovation programme under the Marie Skłodowska-Curie grant agreement No 709175. MK was supported by the National Science Centre, Poland grant no. 2015/19/B/NZ8/03945. NM was supported by ARCEx and the Research Council of Norway (Grant 228107).

### Data Accessibility
The datasets supporting this article have been uploaded to Pangaea. Additional data used in this paper are found in [37,40].

### Competing Interests
We had no competing interests.

### Authors' Contributions
AT and CM were responsible for the design of this project. CM, MK, NM, MN, JM, MO, and IP were involved in sample collection. AT, CM, MK, and NM contributed to data production. All authors contributed to the data interpretation, drafting, revising, and final approval of the manuscript.

# References

1. Perovich D. 2017 Sea ice and sunlight. In *Sea Ice* (ed DN Thomas), pp. 110–137.
2. Spielhagen RF, Werner K, Sorensen SA, Zamelczyk K, Kandiano E, Budeus G, Husum K, Marchitto TM, Hald M. 2011 Enhanced Modern Heat Transfer to the Arctic by Warm Atlantic Water. *Science (80-. ).* **331**, 450–453. (doi:10.1126/science.1197397)
3. Woodgate RA, Weingartner TJ, Lindsay R. 2012 Observed increases in Bering Strait oceanic fluxes from the Pacific to the Arctic from 2001 to 2011 and their impacts on the Arctic Ocean water column. *Geophys. Res. Lett.* **39**, 2012GL054092. (doi:10.1029/2012GL054092)
4. Meredith M *et al.* 2019 Polar regions. In *IPCC Special Report on the Ocean and Cryosphere in a Changing Climate* (eds H-O Pörtner, DC Roberts, V Masson-Delmotte, P Zhai, M Tignor, E

Poloczanska, K Mintenbeck, A Alegría, M Nicolai, A Okem, et al.),
5. Fernández-Méndez M, Katlein C, Rabe B, Nicolaus M, Peeken I, Bakker K, Flores H, Boetius A. 2015 Photosynthetic production in the central Arctic Ocean during the record sea-ice minimum in 2012. *Biogeosciences* **12**, 3525–3549. (doi:10.5194/bg-12-3525-2015)
6. Tremblay J-É, Anderson LG, Matrai P, Coupel P, Bélanger S, Michel C, Reigstad M. 2015 Global and regional drivers of nutrient supply, primary production and CO2 drawdown in the changing Arctic Ocean. *Prog. Oceanogr.* **139**, 171–196. (doi:10.1016/j.pocean.2015.08.009)
7. Arrigo KR, van Dijken GL. 2015 Continued increases in Arctic Ocean primary production. *Prog. Oceanogr.* **136**, 60–70. (doi:10.1016/j.pocean.2015.05.002)
8. Tyrrell T. 1999 The relative influences of nitrogen and phosphorus on oceanic primary production. *Nature* **400**, 525–531. (doi:10.1038/22941)
9. Karl DM. 2014 Microbially Mediated Transformations of Phosphorus in the Sea: New Views of an Old Cycle. *Ann. Rev. Mar. Sci.* **6**, 279–337. (doi:10.1146/annurev-marine-010213-135046)
10. Martiny AC *et al.* 2019 Biogeochemical controls of surface ocean phosphate. *Sci. Adv.* **5**, eaax0341. (doi:10.1126/sciadv.aax0341)
11. Lomas MW, Bonachela JA, Levin SA, Martiny AC. 2014 Impact of ocean phytoplankton diversity on phosphate uptake. *Proc. Natl. Acad. Sci.* **111**, 17540–17545. (doi:10.1073/pnas.1420760111)
12. Froelich PN, Bender ML, Luedtke NA, Heath GR, DeVries T. 1982 The marine phosphorus cycle. *Am. J. Sci.* **282**, 474–511. (doi:10.2475/ajs.282.4.474)
13. Wallmann K. 2010 Phosphorus imbalance in the global ocean? *Global Biogeochem. Cycles* **24**, n/a-n/a. (doi:10.1029/2009GB003643)
14. Torres-Valdés S *et al.* 2013 Export of nutrients from the Arctic Ocean. *J. Geophys. Res. Ocean.* **118**, 1625–1644. (doi:10.1002/jgrc.20063)
15. Carmack E *et al.* 2015 Toward Quantifying the Increasing Role of Oceanic Heat in Sea Ice Loss in the New Arctic. *Bull. Am. Meteorol. Soc.* **96**, 2079–2105. (doi:10.1175/BAMS-D-13-00177.1)
16. Hawkings J *et al.* 2016 The Greenland Ice Sheet as a hot spot of phosphorus weathering and export in the Arctic. *Global Biogeochem. Cycles* **30**, 191–210. (doi:10.1002/2015GB005237)
17. Paytan A, McLaughlin K. 2007 The Oceanic Phosphorus Cycle. *Chem. Rev.* **107**, 563–576. (doi:10.1021/cr0503613)
18. Ruttenberg KC. 2014 The Global Phosphorus Cycle. In *Treatise on Geochemistry*, pp. 499–558. Elsevier. (doi:10.1016/B978-0-08-095975-7.00813-5)
19. Defforey D, Paytan A. 2018 Phosphorus cycling in marine sediments: Advances and challenges. *Chem. Geol.* **477**, 1–11. (doi:10.1016/j.chemgeo.2017.12.002)
20. Bhatia MP, Kujawinski EB, Das SB, Breier CF, Henderson PB, Charette MA. 2013 Greenland meltwater as a significant and potentially bioavailable source of iron to the ocean. *Nat. Geosci.* **6**, 274–278. (doi:10.1038/ngeo1746)
21. Hawkings JR *et al.* 2014 Ice sheets as a significant source of highly reactive nanoparticulate iron to the oceans. *Nat. Commun.* **5**. (doi:10.1038/ncomms4929)
22. Hodson A, Nowak A, Sabacka M, Jungblut A, Navarro F, Pearce D, Ávila-Jiménez ML, Convey P, Vieira G. 2017 Climatically sensitive transfer of iron to maritime Antarctic ecosystems by surface runoff. *Nat. Commun.* **8**, 14499. (doi:10.1038/ncomms14499)
23. Hawkings JR *et al.* 2018 Biolabile ferrous iron bearing nanoparticles in glacial sediments. *Earth Planet. Sci. Lett.* **493**, 92–101. (doi:10.1016/j.epsl.2018.04.022)
24. Nickel M, Vandieken V, Brüchert V, Jørgensen BB. 2008 Microbial Mn(IV) and Fe(III) reduction in northern Barents Sea sediments under different conditions of ice cover and organic carbon deposition. *Deep Sea Res. Part II Top. Stud. Oceanogr.* **55**, 2390–2398. (doi:10.1016/j.dsr2.2008.05.003)
25. HOWE JA, SHIMMIELD TM, HARLAND R. 2007 Late Quaternary contourites and glaciomarine sedimentation in the Fram Strait. *Sedimentology* , 071008041531003-??? (doi:10.1111/j.1365-3091.2007.00897.x)
26. Aagaard K, Swift JH, Carmack EC. 1985 Thermohaline circulation in the Arctic Mediterranean Seas. *J. Geophys. Res.* **90**, 4833. (doi:10.1029/JC090iC03p04833)
27. Coachman LK, Aagaard K. 1974 Physical Oceanography of Arctic and Subarctic Seas. In *Marine Geology and Oceanography of the Arctic Seas*, pp. 1–72. Berlin, Heidelberg: Springer Berlin Heidelberg. (doi:10.1007/978-3-642-87411-6_1)
28. Aagaard K, Foldvik A, Hillman SR. 1987 The West Spitsbergen Current: Disposition and water mass transformation. *J. Geophys. Res.* **92**, 3778. (doi:10.1029/JC092iC04p03778)
29. Muench RD, McPhee MG, Paulson CA, Morison JH. 1992 Winter oceanographic conditions in the Fram Strait-Yermak Plateau region. *J. Geophys. Res.* **97**, 3469. (doi:10.1029/91JC03107)
30. Cokelet ED, Tervalon N, Bellingham JG. 2008 Hydrography of the West Spitsbergen Current, Svalbard Branch: Autumn 2001. *J. Geophys. Res.* **113**, C01006. (doi:10.1029/2007JC004150)
31. Sirevaag A, de la Rosa S, Fer I, Nicolaus M, Tjernström M, McPhee MG. 2011 Mixing, heat fluxes and heat content evolution of the Arctic Ocean mixed layer. *Ocean Sci.* **7**, 335–349. (doi:10.5194/os-

7-335-2011)
32. Saloranta TM, Haugan PM. 2004 Northward cooling and freshening of the warm core of the West Spitsbergen Current. *Polar Res.* **23**, 79–88. (doi:10.3402/polar.v23i1.6268)
33. Peeken I. 2016 The Expedition PS92 of the Research Vessel POLARSTERN to the Arctic Ocean in 2015. *Berichte zur Polar- und Meeresforsch. = Reports polar Mar. Res. Bremerhaven, Alfred Wegener Inst. Polar Mar. Res.* **694**, 153. (doi:10.2312/BzPM_0694_2016)
34. Eckert S, Brumsack H-J, Severmann S, Schnetger B, März C, Fröllje H. 2013 Establishment of euxinic conditions in the Holocene Black Sea. *Geology* **41**, 431–434. (doi:10.1130/G33826.1)
35. Ruttenberg KC. 1992 Development of a sequential extraction method for different forms of phosphorus in marine sediments. *Limnol. Oceanogr.* **37**, 1460–1482. (doi:10.4319/lo.1992.37.7.1460)
36. Thompson J, Poulton SW, Guilbaud R, Doyle KA, Reid S, Krom MD. 2019 Development of a modified SEDEX phosphorus speciation method for ancient rocks and modern iron-rich sediments. *Chem. Geol.* **524**, 383–393. (doi:10.1016/j.chemgeo.2019.07.003)
37. Tessin AC, März C, Blais M-A, Brumsack H, Matthiessen J, O'Regan M, Schnetger B. In press. Arctic continental margin sediments as possible Fe and Mn sources to seawater as sea ice retreats: Insights from the Eurasian Margin. *Global Biogeochem. Cycles*
38. Raiswell R, Vu HP, Brinza L, Benning LG. 2010 The determination of labile Fe in ferrihydrite by ascorbic acid extraction: Methodology, dissolution kinetics and loss of solubility with age and de-watering. *Chem. Geol.* **278**, 70–79. (doi:10.1016/j.chemgeo.2010.09.002)
39. Holm-Hansen O, Lorenzen CJ, Holmes RW, Strickland JDH. 1965 Fluorometric Determination of Chlorophyll. *ICES J. Mar. Sci.* **30**, 3–15. (doi:10.1093/icesjms/30.1.3)
40. Oleszczuk B, Michaud E, Morata N, Renaud PE, Kędra M. 2019 Benthic macrofaunal bioturbation activities from shelf to deep basin in spring to summer transition in the Arctic Ocean. *Mar. Environ. Res.* **150**, 104746. (doi:10.1016/j.marenvres.2019.06.008)
41. Oleszczuk B, K G, M K. In press. Arctic benthic fauna community structure and productivity across depth gradients during spring time. *Deep Sea Res. I*
42. Seeberg-Elverfeldt J, Schlüter M, Feseker T, Kölling M. 2005 Rhizon sampling of porewaters near the sediment-water interface of aquatic systems. *Limnol. Oceanogr. Methods* **3**, 361–371. (doi:10.4319/lom.2005.3.361)
43. März C, Meinhardt A-K, Schnetger B, Brumsack H-J. 2015 Silica diagenesis and benthic fluxes in the Arctic Ocean. *Mar. Chem.* **171**, 1–9. (doi:10.1016/j.marchem.2015.02.003)
44. Ullman WJ, Aller RC. 1982 Diffusion coefficients in nearshore marine sediments1. *Limnol. Oceanogr.* **27**, 552–556. (doi:10.4319/lo.1982.27.3.0552)
45. Ingall ED, Bustin RM, Van Cappellen P. 1993 Influence of water column anoxia on the burial and preservation of carbon and phosphorus in marine shales. *Geochim. Cosmochim. Acta* **57**, 303–316. (doi:10.1016/0016-7037(93)90433-W)
46. Jensen HS, Mortensen PB, Andersen F., Rasmussen E, Jensen A. 1995 Phosphorus cycling in a coastal marine sediment, Aarhus Bay, Denmark. *Limnol. Oceanogr.* **40**, 908–917. (doi:10.4319/lo.1995.40.5.0908)
47. Canfield DE, Erik Kristensen, Bo Thamdrup. 2005 The Phosphorus Cycle. pp. 419–440. (doi:10.1016/S0065-2881(05)48011-6)
48. Ruttenberg KC, Berner RA. 1993 Authigenic apatite formation and burial in sediments from non-upwelling, continental margin environments. *Geochim. Cosmochim. Acta* **57**, 991–1007. (doi:10.1016/0016-7037(93)90035-U)
49. Berner RA. 1973 Phosphate removal from sea water by adsorption on volcanogenic ferric oxides. *Earth Planet. Sci. Lett.* **18**, 77–86. (doi:10.1016/0012-821X(73)90037-X)
50. Colombo C, Barrón V, Torrent J. 1994 Phosphate adsorption and desorption in relation to morphology and crystal properties of synthetic hematites. *Geochim. Cosmochim. Acta* **58**, 1261–1269. (doi:10.1016/0016-7037(94)90380-8)
51. Slomp CP, Epping EHG, Helder W, Raaphorst W Van. 1996 A key role for iron-bound phosphorus in authigenic apatite formation in North Atlantic continental platform sediments. *J. Mar. Res.* **54**, 1179–1205. (doi:10.1357/0022240963213745)
52. Anschutz P, Zhong S, Sundby B, Mucci A, Gobeil C. 1998 Burial efficiency of phosphorus and the geochemistry of iron in continental margin sediments. *Limnol. Oceanogr.* **43**, 53–64. (doi:10.4319/lo.1998.43.1.0053)
53. Dybwad C. 2016 Fate of production in the Arctic seasonal ice zone. The Arctic University of Norway.
54. Meyer A, Fer I, Sundfjord A, Peterson AK. 2017 Mixing rates and vertical heat fluxes north of Svalbard from Arctic winter to spring. *J. Geophys. Res. Ocean.* **122**, 4569–4586. (doi:10.1002/2016JC012441)
55. Reigstad M, Carroll J, Slagstad D, Ellingsen I, Wassmann P. 2011 Intra-regional comparison of productivity, carbon flux and ecosystem composition within the northern Barents Sea. *Prog. Oceanogr.* **90**, 33–46. (doi:10.1016/j.pocean.2011.02.005)

56. Svensen C, Halvorsen E, Vernet M, Franzè G, Dmoch K, Lavrentyev PJ, Kwasniewski S. 2019 Zooplankton Communities Associated With New and Regenerated Primary Production in the Atlantic Inflow North of Svalbard. *Front. Mar. Sci.* **6**. (doi:10.3389/fmars.2019.00293)
57. Kowalczuk P, Meler J, Kauko HM, Pavlov AK, Zabłocka M, Peeken I, Dybwad C, Castellani G, Granskog MA. 2017 Bio-optical properties of Arctic drift ice and surface waters north of Svalbard from winter to spring. *J. Geophys. Res. Ocean.* **122**, 4634–4660. (doi:10.1002/2016JC012589)
58. Froelich PN *et al.* 1979 Early oxidation of organic matter in pelagic sediments of the eastern equatorial Atlantic: suboxic diagenesis. *Geochim. Cosmochim. Acta* **43**, 1075–1090. (doi:10.1016/0016-7037(79)90095-4)
59. Chen C, Sparks DL. 2018 Fe(II)-Induced Mineral Transformation of Ferrihydrite–Organic Matter Adsorption and Co-precipitation Complexes in the Absence and Presence of As(III). *ACS Earth Sp. Chem.* **2**, 1095–1101. (doi:10.1021/acsearthspacechem.8b00041)
60. Tessenow VU. In press. Solution, diffusion and sorption in the upper layer of lake sediments. IV. Reaction mechanisms and equilibria in the system iron-manganese-phosphate with regard to the accumulation of vivianite in Lake Ursee. *Arch. für Hydrobiol. , Suppl.* **47**, 1–79.
61. Tejedor-Tejedor MI, Anderson MA. 1990 The protonation of phosphate on the surface of goethite as studied by CIR-FTIR and electrophoretic mobility. *Langmuir* **6**, 602–611. (doi:10.1021/la00093a015)
62. Golterman HL. 1995 Theoretical aspects of the adsorption of ortho-phosphate onto iron-hydroxide. *Hydrobiologia* **315**, 59–68. (doi:10.1007/BF00028630)
63. Gunnars A, Blomqvist S, Johansson P, Andersson C. 2002 Formation of Fe(III) oxyhydroxide colloids in freshwater and brackish seawater, with incorporation of phosphate and calcium. *Geochim. Cosmochim. Acta* **66**, 745–758. (doi:10.1016/S0016-7037(01)00818-3)
64. Vancoppenolle M, Bopp L, Madec G, Dunne J, Ilyina T, Halloran PR, Steiner N. 2013 Future Arctic Ocean primary productivity from CMIP5 simulations: Uncertain outcome, but consistent mechanisms. *Global Biogeochem. Cycles* **27**, 605–619. (doi:10.1002/gbc.20055)
65. Slagstad D, Wassmann PFJ, Ellingsen I. 2015 Physical constrains and productivity in the future Arctic Ocean. *Front. Mar. Sci.* **2**. (doi:10.3389/fmars.2015.00085)
66. Raiswell R, Tranter M, Benning LG, Siegert M, De'ath R, Huybrechts P, Payne T. 2006 Contributions from glacially derived sediment to the global iron (oxyhydr)oxide cycle: Implications for iron delivery to the oceans. *Geochim. Cosmochim. Acta* **70**, 2765–2780. (doi:10.1016/j.gca.2005.12.027)

## Tables

**Table 1.** Locations of cores in this study. Full site names are given here, and shortened in the text to the station name (i.e. for the first core in the table 19) and deployment number (i.e. for the first core in the table 19).

| Core | Water depth (m) | Latitude | Longitude |
|---|---|---|---|
| ***Barents Sea slope*** | | | |
| PS92/019-19-MC | 481 | 81° 13.79' N | 18° 33.04' E |
| PS92/027-15-MC | 795 | 81° 19.55' N | 17° 16.87' E |
| PS92/031-13-MC | 1852 | 81° 30.20' N | 18° 31.72' E |
| ***Sophia Basin*** | | | |
| PS92/047-20-MC | 2175 | 81° 20.68' N | 13° 39.94' E |
| ***Yermak Plateau (eastern flank)*** | | | |
| PS92/039-05-MC | 1523 | 81° 55.50' N | 13° 37.98' E |
| PS92/040-01-MC | 1158 | 81° 49.04' N | 10° 52.06' E |
| PS92/046-15-MC | 886 | 81° 50.62' N | 09° 45.48' E |
| PS92/056-05-MC | 854 | 81° 0.94' N | 08° 17.05' E |
| ***Yermak Plateau (western flank)*** | | | |
| PS92/043-20-MC | 817 | 82° 10.45' N | 07° 0.53' E |

**Table 2.** Concentrations of (a) Chl *a* (μg/g) in the surface sediments, (b) maximum Fe bound P (weight %), and (c) maximum Fe bound P/total P. Dashes are used to indicate no existing data.

| Core | Chl *a* | Max $P_{Fe}$ (wt.%) | $P_{Fe}/P_{Tot}$(%) |
|---|---|---|---|
| ***Barents Sea slope*** | | | |
| 19-19 | 0.71 | 0.034 | 13.7 |
| 27-15 | 0.64 | 0.005 | 7.4 |
| 31-13 | 0.27 | 0.004 | - |

| | | | |
|---|---|---|---|
| *Sophia Basin* | | | |
| 47-20 | 0.10 | 0.008 | - |
| *Yermak Plateau (eastern flank)* | | | |
| 39-5 | 0.09 | 0.007 | 7.6 |
| 40-1 | - | 0.008 | - |
| 46-15 | 0.08 | 0.007 | 7.2 |
| 56-5 | - | 0.007 | 7.6 |
| *Yermak Plateau (western flank)* | | | |
| 43-20 | 0.04 | 0.008 | - |

**Table 3.** Calculated diffusive fluxes for the studied cores. Fluxes into bottom waters are bolded and fluxes into a near surface sediment layer are italicized.

| Core | Water depth (m) | Diffusive Flux ($\mu$mol m$^{-2}$ yr$^{-1}$) |
|---|---|---|
| *Barents Sea slope* | | |
| PS92/019-19-MC | 481 | *2449* |
| PS92/027-15-MC | 795 | *1996* |
| PS92/031-13-MC | 1852 | *1736* |
| *Sophia Basin* | | |
| PS92/047-20-MC | 2175 | **117** |
| *Yermak Plateau (eastern flank)* | | |
| PS92/039-05-MC | 1523 | **189** |
| PS92/040-01-MC | 1158 | **141** |
| PS92/046-15-MC | 886 | **96** |
| PS92/056-05-MC | 854 | **261** |
| *Yermak Plateau (western flank)* | | |
| PS92/043-20-MC | 817 | **151** |



## Figure captions

Figure 1. Map of the Barents Sea and Eurasian Arctic margin (adapted from Tessin et al., in review). Cores are indicated with circles (Yermak Plateau core in yellow, Sofia Basin core in orange and Barents Sea slope cores in red). Median sea ice extent from 1981-2010 for March (dashed) and September (solid) are indicated in yellow (data from the National Snow and Ice Data Center, www.nsidc.org). Bathymetry is indicated by shades of blue (Jakobsson et al., 2003).The West Spitsbergen Current is indicated in red.

Figure 2. Downcore records of (a) P/Al (%/%) and (b) P/Fe (%/%) from XRF analysis. Dashed lines indicate average shale ratio of 0.008. Barents Sea slope sites (19-19 and 27-15) are in red and Yermak Plateau sites (39-5, 46-15, and 56-5) are in yellow.

Figure 3. Downcore records of (a) organic carbon to phosphorus (C/P) ratios (%/%) and (b) total organic carbon (TOC). Barents Sea slope sites (19-19 and 27-15) are in red and Yermak Plateau sites (39-5, 46-15, and 56-5) are in yellow.

Figure 4. Crossplot of Ascorbic extractable Fe (from Tessin et al., in revision) vs. Fe-bound P. Sediments from the Barents Sea slope are in red, Sofia Basin are in orange, and the Yermak Plateau are in yellow. Slope lines for the Barents Sea slope cores and the Yermak Plateau cores are included as dashed lines. The slope for the Sofia Basin core (47-20) is similar to the Yermak Plateau slope but not shown.

**Figure 5**. Records of (a) porewater phosphorus and (b) porewater iron to phosphorus ratios. Barents Sea slope sites (19-19 and 27-15) are in red and Yermak Plateau sites (39-5, 46-15, and 56-5) are in orange. Blue squares represent bottom water samples. Orange horizontal lines represent transition porewater iron reduction and precipitation (Tessin et al., in revision).

**Figure 6**. Geochemical results from the Eurasian Arctic Margin including (a) surface chl *a* values in core top sediments, (b) total organic carbon in core top sediments, (c) diffusive flux of P, and (d) Ratio of Fe-bound P and ascorbate extractable Fe in core top sediments.

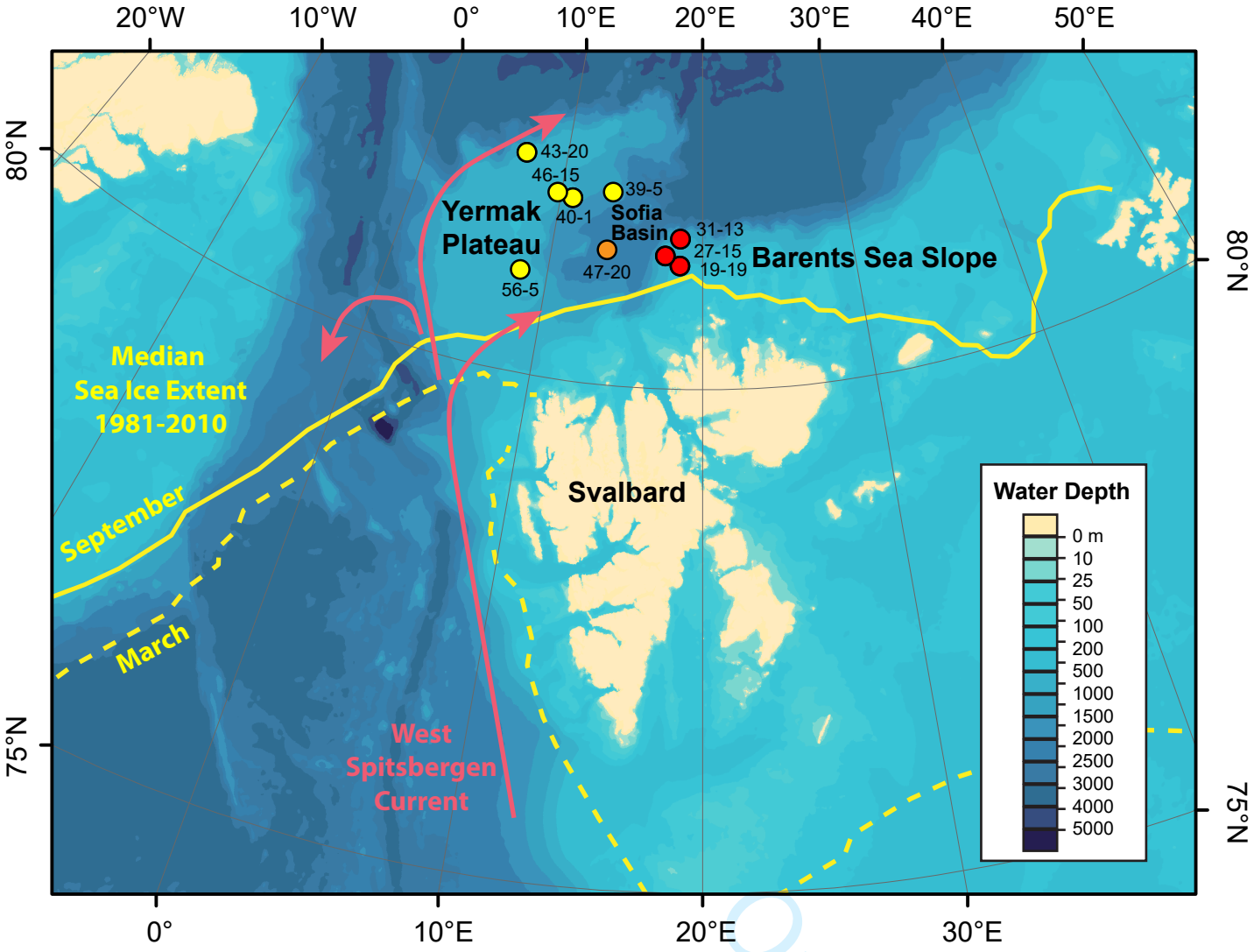


**Figure 1**. Map of the Barents Sea and Eurasian Arctic margin (adapted from Tessin et al., in review). Cores are indicated with circles (Yermak Plateau core in yellow, Sofia Basin core in orange and Barents Sea slope cores in red). Median sea ice extent from 1981-2010 for March (dashed) and September (solid) are indicated in yellow (data from the National Snow and Ice Data Center, www.nsidc.org). Bathymetry is indicated by shades of blue (Jakobsson et al., 2003). The West Spitsbergen Current is indicated in red.

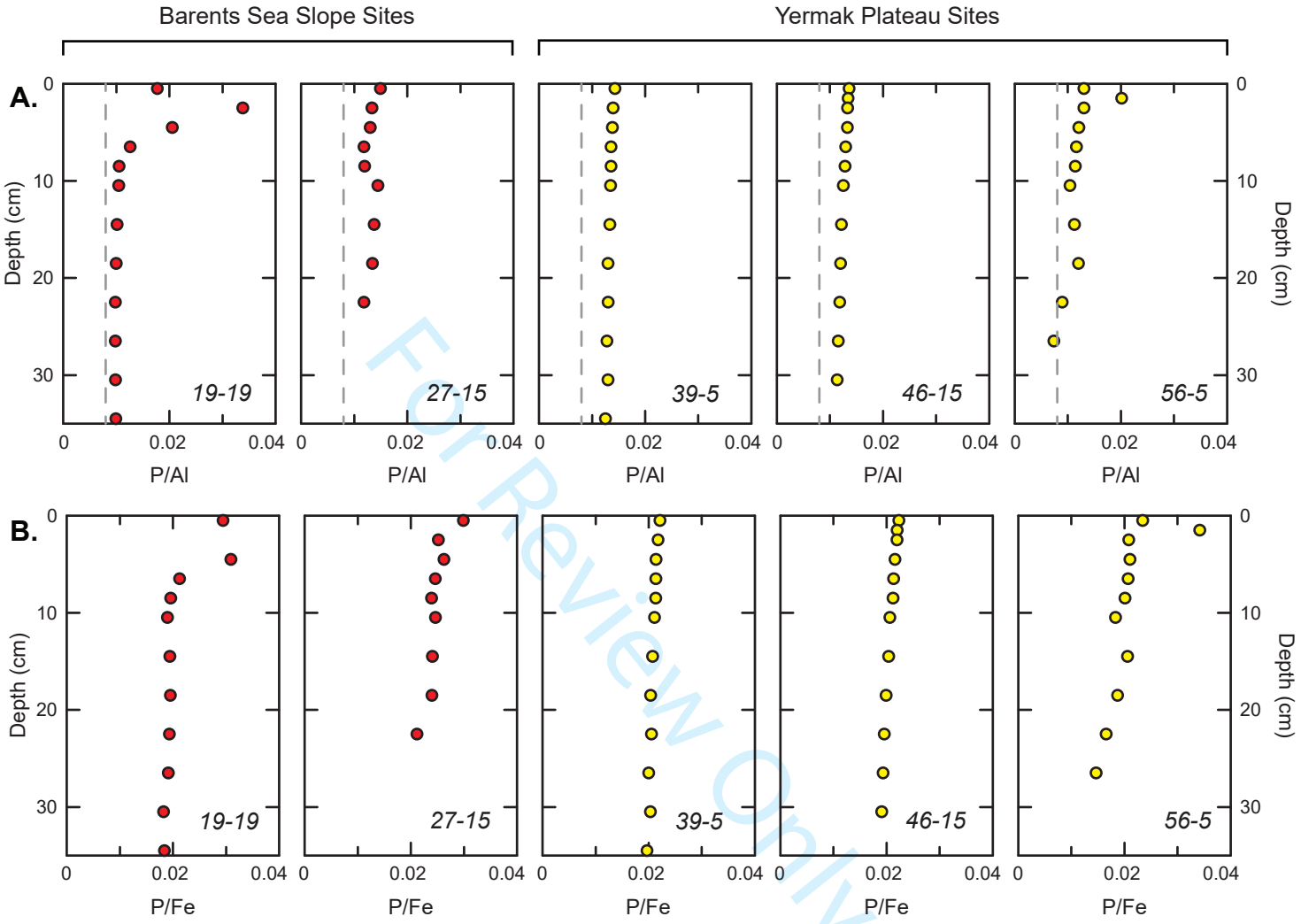


**Figure 2**. Downcore records of (a) P/Al (%/%) and (b) P/Fe (%/%) from XRF analysis. Dashed lines indicate average shale ratio of 0.008. Barents Sea slope sites (19-19 and 27-15) are in red and Yermak Plateau sites (39-5, 46-15, and 56-5) are in yellow.

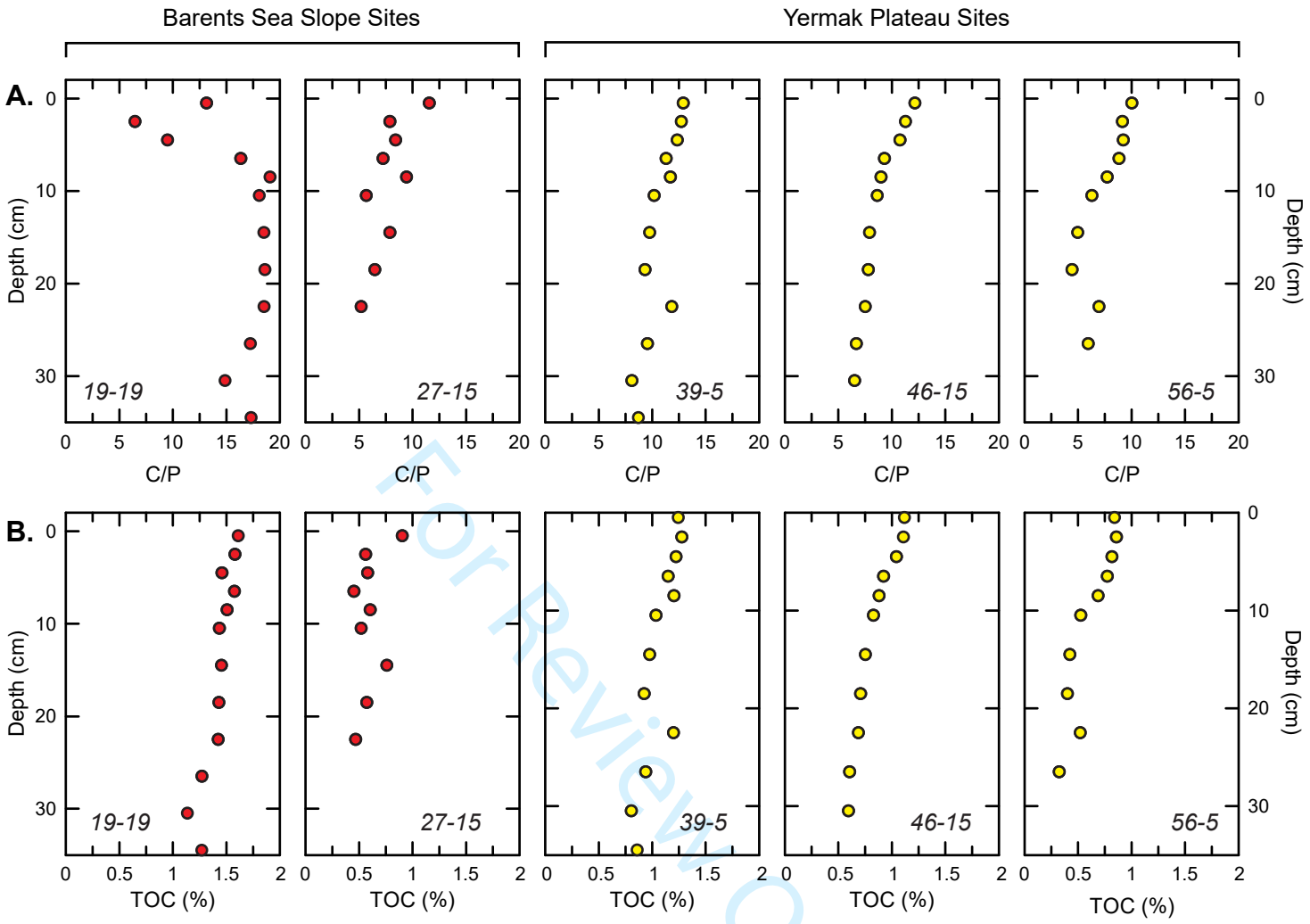


**Figure 3**. Downcore records of (a) organic carbon to phosphorus (C/P) ratios (%/%) and (b) total organic carbon (TOC). Barents Sea slope sites (19-19 and 27-15) are in red and Yermak Plateau sites (39-5, 46-15, and 56-5) are in yellow.

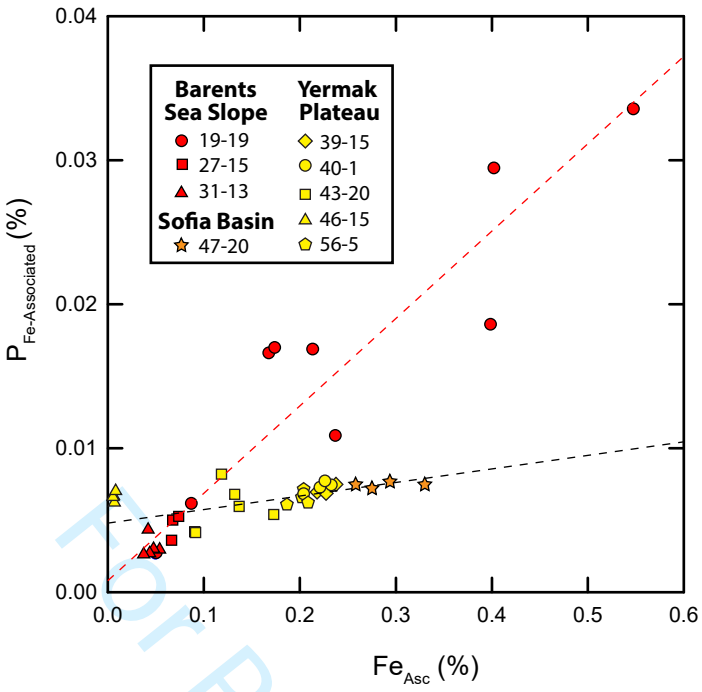


**Figure 4**. Crossplot of Ascorbic extractable Fe (from Tessin et al., in revision) vs. Fe-bound P. Sediments from the Barents Sea slope are in red, Sofia Basin are in orange, and the Yermak Plateau are in yellow. Slope lines for the Barents Sea slope cores and the Yermak Plateau cores are included as dashed lines. The slope for the Sofia Basin core (47-20) is similar to the Yermak Plateau slope but not shown.

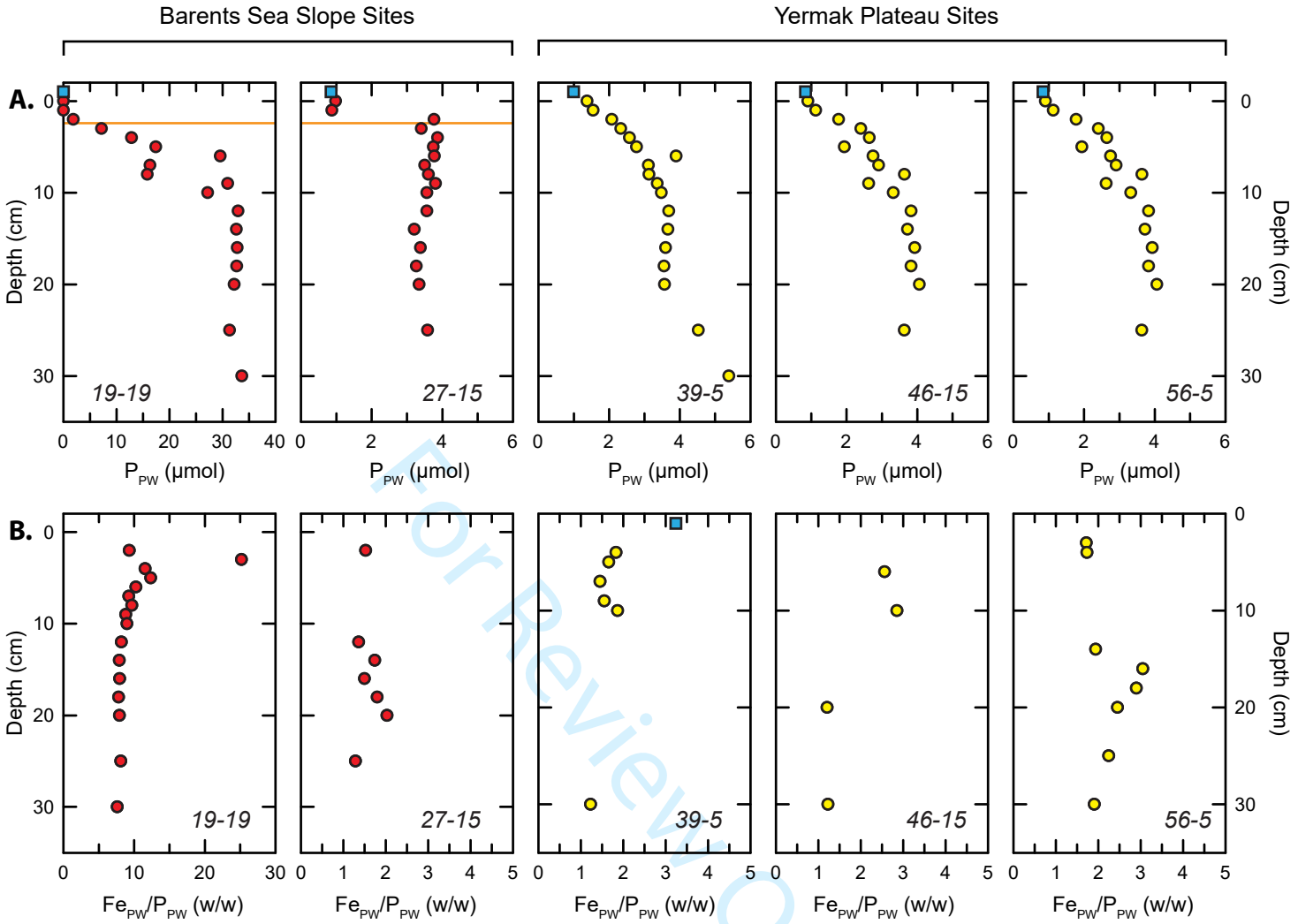


**Figure 5**. Records of (a) porewater phosphorus and (b) porewater iron to phosphorus ratios. Barents Sea slope sites (19-19 and 27-15) are in red and Yermak Plateau sites (39-5, 46-15, and 56-5) are in orange. Blue squares represent bottom water samples. Orange horizontal lines represent transition porewater iron reduction and precipitation (Tessin et al., in revision).

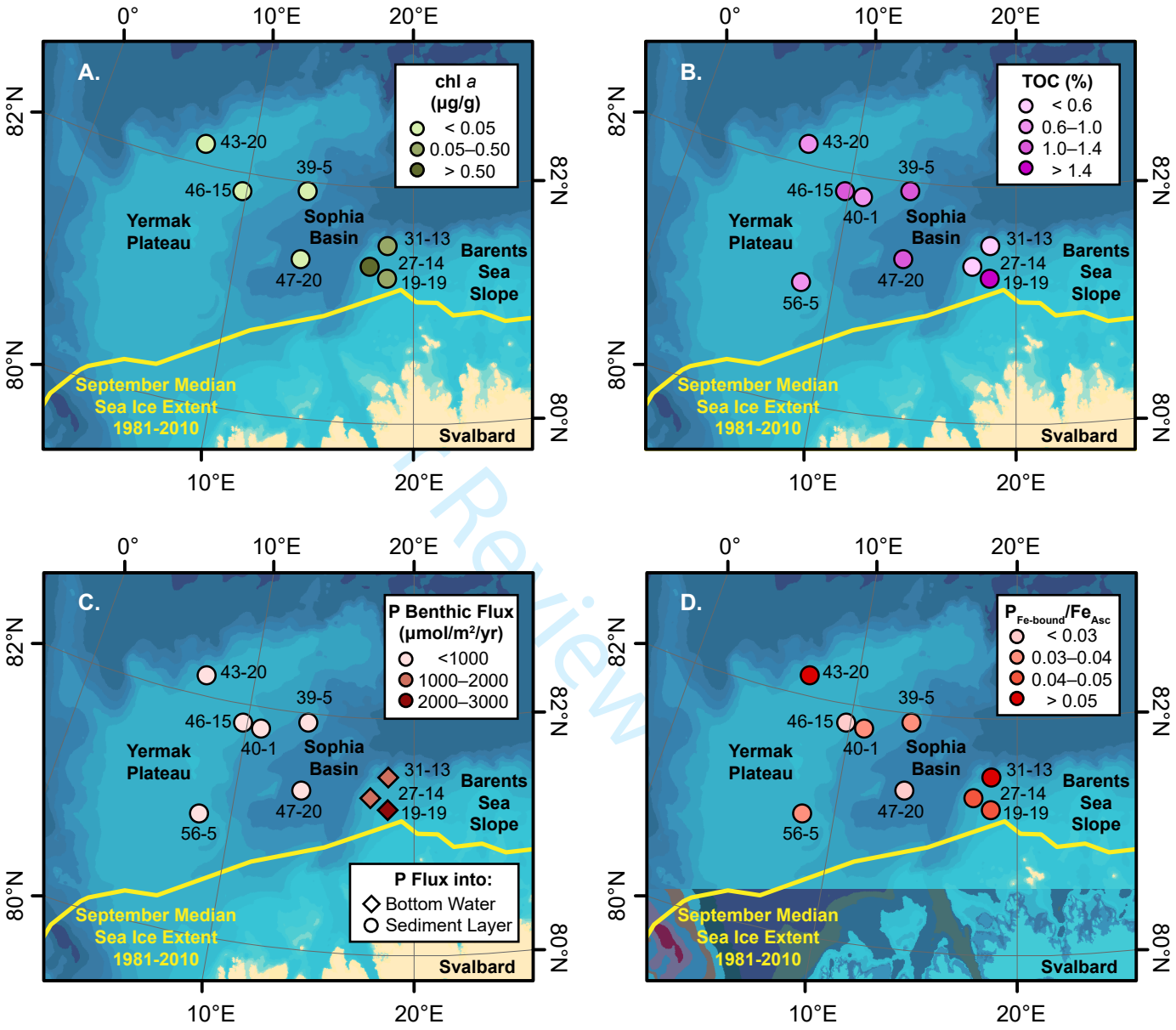


**Figure 6**. Geochemical results from the Eurasian Arctic Margin including (a) surface chl avalues in core top sediments, (b) total organic carbon in core top sediments, (c) diffusive flux of P, and (d) Ratio of Fe-bound P and ascorbate extractable Fe in core top sediments.